



ELSEVIER

Carbohydrate Research 337 (2002) 549–555

CARBOHYDRATE  
RESEARCH

www.elsevier.com/locate/carres

# Monte Carlo docking simulations of cyclomaltoheptaose and dimethyl cyclomaltoheptaose with paclitaxel

Hyunmyung Kim,<sup>a</sup> Jungwon Choi,<sup>b</sup> Hyun-Won Kim,<sup>c</sup> Seunho Jung<sup>a,\*</sup><sup>a</sup>Department of Microbial Engineering, Konkuk University, 1 Hwayang-dong, Gwangjin-gu, Seoul 143-701, South Korea<sup>b</sup>Department of Chemistry, The University of Suwon, San 2-2 Wawoo-ri, Bongdam-eup, Hwasung city, Kyunggi 445-743, South Korea<sup>c</sup>Department of Biochemistry and Institute of Basic Medical Sciences and Medical Engineering Institute, Yonsei University, Wonju College of Medicine, Wonju 220-701, South Korea

Received 15 October 2001; accepted 4 January 2002

## Abstract

The molecular basis for the remarkable enhancement of the solubility of paclitaxel by *O*-dimethylcyclomaltoheptaose (DM- $\beta$ -CD) over cyclomaltoheptaose ( $\beta$ -cyclodextrin,  $\beta$ -CD) was investigated with Monte Carlo docking–minimization simulation. As possible guests of inclusion complexation for the host cyclic oligosaccharides, two functional moieties of the suggested solution structure of paclitaxel were used where one is the C-3'N benzoyl moiety (B-ring) and the other is a hydrophobic (HP) cluster site among the C-3' phenyl (C-ring), C-2 benzoate (A-ring), and C-4 acetoxy moieties. The energetic preference of inclusion complexation of DM- $\beta$ -CD over  $\beta$ -CD was analyzed on the basis of more efficient partitioning process of DM- $\beta$ -CD into the hydrophobic cluster site of the paclitaxel. © 2002 Elsevier Science Ltd. All rights reserved.

**Keywords:** Paclitaxel; Cyclomaltoheptaose ( $\beta$ -CD); *O*-Dimethylcyclomaltoheptaose (DM- $\beta$ -CD); Monte Carlo docking; Solubility

## 1. Introduction

Paclitaxel (Fig. 1) is a diterpenoid natural product of the Pacific yew (*Taxus brevifolia*)<sup>1</sup> showing encouraging activity against ovarian, breast, head and neck, and non-small-cell lung cancers.<sup>2</sup> It binds to the  $\beta$ -tubulin

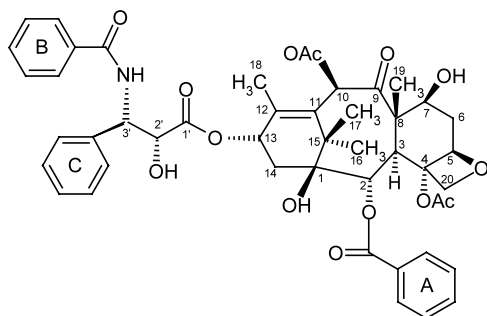


Fig. 1. Chemical structure of paclitaxel with numbering scheme.

binding site on microtubules, promotes their assembly from tubulin heterodimers, and stabilizes them against depolymerization. The resulting abnormal tubulin–microtubule equilibrium disrupts the normal mitotic spindle apparatus, which underlies the ability of paclitaxel to block cell proliferation at the tetraploid G<sub>2</sub>-M phases of the cell cycle.<sup>3</sup> Recently paclitaxel has been approved in the form of Taxol for treatment of breast and refractory human ovarian cancer. One of the major problems with paclitaxel therapy arises from the extremely low-aqueous solubility of the drug.<sup>4</sup> In order to circumvent this problem, several trials such as encapsulation by liposomes, organic solvent formulation with polyethoxylated castor oil, and complexation with solubilizing agents have been performed.<sup>5–7</sup> One of the latter is to use the inclusion complex of paclitaxel with cyclic oligosaccharides like cyclodextrins.<sup>8</sup> Cyclodextrins (CDs) are cyclic oligosaccharides consisting of covalently linked glucopyranose rings. CDs ( $\alpha$ -,  $\beta$ -, and  $\gamma$ -CD) have been used extensively to increase the aqueous solubility of drugs<sup>9,10</sup> and to increase the stability of labile drugs.<sup>11,12</sup> CDs were modified chemically or enzymatically to improve their aqueous solubility or

\* Corresponding author. Tel./fax: + 82-2-4503520.

E-mail address: [shjung@konkuk.ac.kr](mailto:shjung@konkuk.ac.kr) (S. Jung).

modulate their toxicity. The property of enhancing solubility and stability derives from the formation of a water-soluble inclusion complex, in which the hollow, truncated, cone-like CD structure encapsulates and shields hydrophobic or labile drug molecules in the electron-rich, apolar interior, while the outer, hydrophilic region of the CDs enables solubilization through interaction with water molecules.<sup>13</sup> *O*-Dimethylcyclomaltoheptaose (DM- $\beta$ -CD) was demonstrated to be the most efficient solubilizing agent for paclitaxel.<sup>14</sup> DM- $\beta$ -CD enhanced paclitaxel solubility by approximately 100,000-fold<sup>5</sup> comparing about tenfold of 1.5%  $\beta$ -cyclodextrin ( $\beta$ -CD).<sup>7</sup> This remarkable difference of solubility was not completely understood at the molecular level. In the present paper, we investigated the inclusion complexation of paclitaxel with  $\beta$ -CD and DM- $\beta$ -CD based on computational calculations. The preferential solubility enhancement of paclitaxel by DM- $\beta$ -CD was scrutinized by the Monte Carlo docking–minimization method.

## 2. Results and discussion

The Monte Carlo (MC) docking simulations showed general tendencies of inclusion complex formation and lowering interaction energies for both CDs with paclitaxel. The interaction energy was defined as the difference between the sum of the independently calculated energy of each host–guest molecule and the energy of each configuration in the process of MC docking simulations.<sup>15</sup> In the process of MC docking simulation, CDs were considered as ligands and paclitaxel as a receptor molecule. During the simulations, the whole coordinates of CDs were flexible. Two different binding sites of the solution structure of paclitaxel were assumed, where one was the C-3'N benzoyl (B-ring) moiety and the other was the hydrophobic (HP) cluster among the C-3' phenyl, C-2 benzoate and C-4 acetoxy moieties (Fig. 2(A)). These assumptions were based on the recent report by Ojima et al. who reported that this hydrophobic cluster played a significant role in the conformational equilibrium of paclitaxel.<sup>16</sup> Fig. 2 shows the molecular models used in this MC docking simulations. MC docking simulations were performed in a vacuum and with an implicit solvent system where the dielectric constant was set to 1 and  $r$ , respectively. The distance-dependent dielectric constant ( $\epsilon = r$ ) was used to simulate solvent water.<sup>17</sup> Fig. 3 compares each of the interaction energies obtained after the MC runs. After 1000 trials, interaction energies reached an equilibrium value and fluctuated around it in a stable manner. Therefore, we considered these states ( $> 1000$ ) an equilibrium status, and the average energy was calculated based on this status.

In  $\epsilon = 1$ , the interaction energy of DM- $\beta$ -CD with the B-ring of paclitaxel was slightly lower than that of  $\beta$ -CD (B-ring docking). The average interaction energy of the  $\beta$ -CD–paclitaxel complex was  $-249.6 \pm 1.4$  kcal/mol, and that of the DM- $\beta$ -CD–paclitaxel complex was  $-251.0 \pm 1.9$  kcal/mol in the equilibrium state. However, the interaction energy of DM- $\beta$ -CD with the HP cluster of paclitaxel was much lower than that of the  $\beta$ -CD (HP cluster docking). The average interaction energy of the  $\beta$ -CD–paclitaxel complex was  $-236.5 \pm 1.7$  kcal/mol, and that of the DM- $\beta$ -CD–paclitaxel complex was  $-243.2 \pm 1.0$  kcal/mol in the equilibrium state. The difference of interaction energy between the DM- $\beta$ -CD–paclitaxel complex and the  $\beta$ -CD–paclitaxel complex is  $-6.7 \pm 2.0$  kcal/mol. In the case of  $\epsilon = r$ , the interaction energy difference of the HP cluster docking was similar to that in  $\epsilon = 1$ . The difference of interaction energy between the DM- $\beta$ -CD–paclitaxel complex and the  $\beta$ -CD–paclitaxel complex is  $-6.4 \pm 1.9$  kcal/mol. However, the interaction energy difference of B-ring docking was higher than that in  $\epsilon = 1$ . The difference of interaction energy between the DM- $\beta$ -CD–paclitaxel complex and the  $\beta$ -CD–paclitaxel complex is  $-4.6 \pm 1.9$  kcal/mol in  $\epsilon = r$  compared with the value of  $-1.3 \pm 2.4$  kcal/mol in  $\epsilon = 1$ . These results are summarized in Table 1.

We tried several MC runs from different initial configurations for each CD and obtained similar results (data not shown).

Figs. 4 and 5 each show the lowest energy configurations among the inclusion complexes of  $\beta$ -CD and DM- $\beta$ -CD with paclitaxel. When all the configurations in an equilibrium state were superimposed by a least-squares fitting, the RMSD calculated all over non-hydrogen atoms were only of the order of 1 Å. Thus, each of the lowest energy configurations safely represents the overall feature of inclusion complexes. When compared with  $\beta$ -CD, DM- $\beta$ -CD made a complex with the HP cluster of paclitaxel at a deeper site in the cavity due to the effective partitioning of the dimethyl groups of DM- $\beta$ -CD into the HP cluster site. The center of geometry was moved into a deeper position inside the cavity of DM- $\beta$ -CD. This shift of center of geometry is shown in Table 2. It shows the comparison of the average distance between the center of geometry of the CDs and paclitaxel during the HP cluster docking simulations. DM- $\beta$ -CD was located closer to the HP cluster of paclitaxel than  $\beta$ -CD. In other words, DM- $\beta$ -CD made a more compact complex with paclitaxel than  $\beta$ -CD did, whereby this compactness endowed more favorable van der Waals interaction, thus explaining the formation of a stable inclusion complex. Table 2 also shows the radius of gyration ( $R_G$ ) of the HP cluster site of paclitaxel. DM- $\beta$ -CD led to an increase in the  $R_G$  of the HP cluster more effectively than  $\beta$ -CD after the complexation. These results suggest that DM- $\beta$ -CD

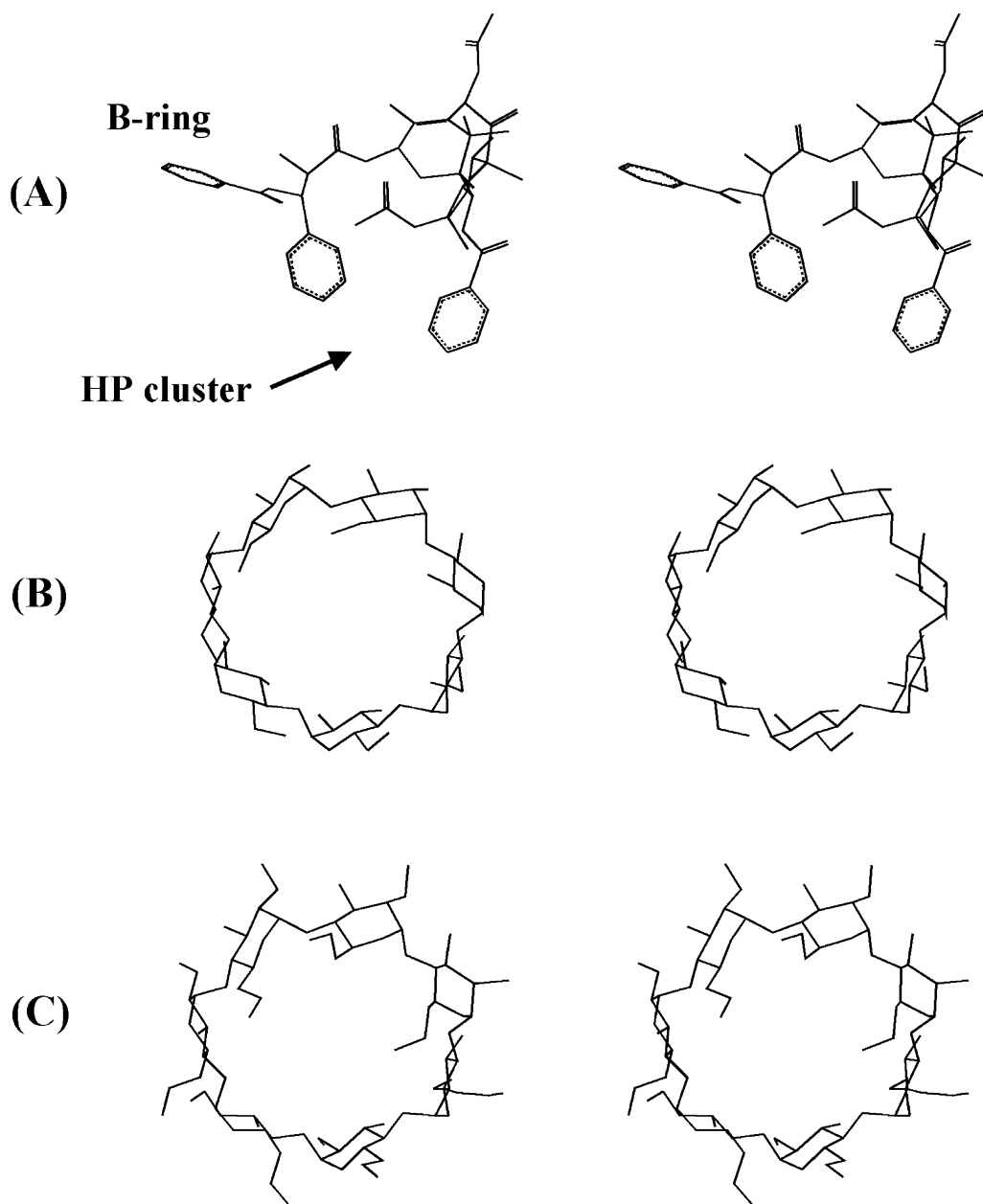


Fig. 2. Stereoview of molecular models used in the MC simulations. (A) Paclitaxel, (B)  $\beta$ -CD, and (C) DM- $\beta$ -CD. Conformation of paclitaxel based on the proposed structure where the H-2'-C-2'-C-3'-H-3' dihedral angle of this conformation is  $124^\circ$ .<sup>16</sup> It has the hydrophobic cluster among the C-3' phenyl, C-2 benzoate and C-4 acetoxy moieties.

may break the hydrophobic cluster within the paclitaxel more efficiently than  $\beta$ -CD, and thus enhance the solubility of paclitaxel. This somewhat effective partitioning of DM- $\beta$ -CD into the hydrophobic cluster moiety of paclitaxel explains why the paclitaxel can be favorably solubilized in the presence of DM- $\beta$ -CD.

Table 1 shows the interaction energy profile of each MC docking in detail. Van der Waals energy seems to be the major contribution to the stability of inclusion complex in both cases. Especially, the contribution of the van der Waals energy term in the HP cluster

docking was much higher in the DM- $\beta$ -CD–paclitaxel complex than in the  $\beta$ -CD–paclitaxel complex, suggesting that the dimethyl groups of DM- $\beta$ -CD played a critical role of inducing the stable inclusion complex.

Throughout this research, MC docking simulation was applied to the investigation for the paclitaxel complexation with two different CDs in terms of the differences in the interaction energies and configuration of inclusion complexes. We propose that the effective partitioning by DM- $\beta$ -CD over  $\beta$ -CD would be the decisive factor for the solubility enhancement of paclitaxel.

Furthermore, these results will also provide very useful information on the future design of more effective complexing agents to enhance paclitaxel solubility. Further researches for the development of novel CD derivatives will be needed in this respect.

### 3. Experimental

Molecular mechanics calculations were performed with the INSIGHTII/DISCOVER program (version 2000, Molecular Simulations Inc., San Diego, USA) using the

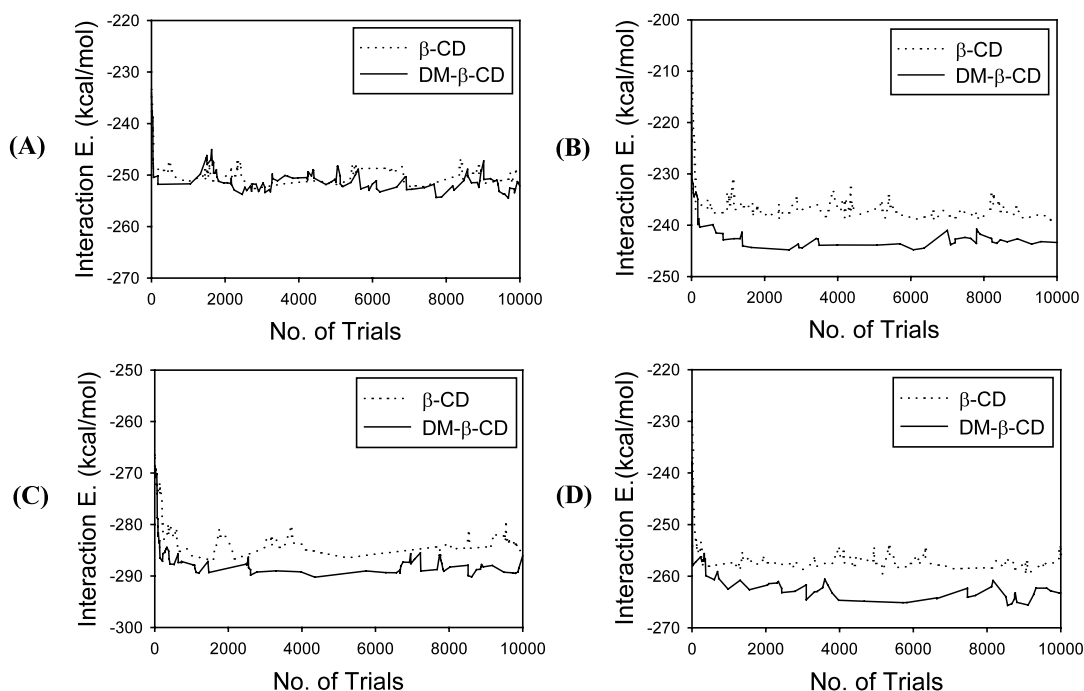


Fig. 3. Energy profile of the Metropolis Monte Carlo docking simulations. The interaction energy was defined as the difference between the sum of independently calculated energy of each host–guest molecule and the energy of each configuration in the process of MC docking simulations. The simulation was performed in  $\varepsilon = 1$ : (A) B-ring; (B) HP cluster; and in  $\varepsilon = r$ : (C) B-ring; (D) HP cluster.

Table 1  
Average interaction energies of the MC docking simulations in equilibrium state

	Docking	Complex	Internal $E^a$	vdW $E^b$	Electro $E$	Total $E^c$
$\varepsilon = 1$	B ring docking	$\beta$ -CD	$-139.9 \pm 1.4$	$-149.2 \pm 1.8$	$39.5 \pm 2.5$	$-249.6 \pm 1.4$
		DM- $\beta$ -CD	$-140.2 \pm 1.9$	$-158.6 \pm 3.3$	$47.9 \pm 1.8$	$-251.0 \pm 1.9$
	$\Delta E^d$		$-0.3 \pm 2.6$	$-9.4 \pm 4.1$	$8.4 \pm 2.8$	$-1.3 \pm 2.4$
	HP cluster docking	$\beta$ -CD	$-122.1 \pm 1.1$	$-126.1 \pm 2.5$	$11.7 \pm 2.0$	$-236.5 \pm 1.7$
		DM- $\beta$ -CD	$-120.3 \pm 1.4$	$-140.5 \pm 1.9$	$17.7 \pm 1.0$	$-243.2 \pm 1.0$
	$\Delta E^d$		$1.8 \pm 1.8$	$-14.4 \pm 3.1$	$6.0 \pm 2.2$	$-6.7 \pm 2.0$
$\varepsilon = r$	B ring docking	$\beta$ -CD	$-143.8 \pm 1.7$	$-151.4 \pm 3.2$	$11.6 \pm 3.3$	$-283.6 \pm 1.5$
		DM- $\beta$ -CD	$-145.6 \pm 1.1$	$-157.3 \pm 2.0$	$14.6 \pm 1.9$	$-288.2 \pm 1.2$
	$\Delta E$		$-1.8 \pm 2.0$	$-5.9 \pm 3.8$	$3.0 \pm 3.8$	$-4.6 \pm 1.9$
	HP cluster docking	$\beta$ -CD	$-125.7 \pm 1.2$	$-127.4 \pm 3.2$	$-3.8 \pm 3.7$	$-256.8 \pm 1.3$
		DM- $\beta$ -CD	$-126.0 \pm 1.0$	$-136.3 \pm 2.2$	$-0.9 \pm 1.8$	$-263.2 \pm 1.4$
	$\Delta E$		$-0.3 \pm 1.6$	$-8.9 \pm 3.9$	$2.9 \pm 4.1$	$-6.4 \pm 1.9$

<sup>a</sup> Internal  $E$  is summation of the energy of deformation bond length, the bond angle, and the dihedral angles.

<sup>b</sup> vdW  $E$  is summation of the repulsive and dispersive van der Waals energy.

<sup>c</sup> Total  $E$  is summation of Internal  $E$  and nonbond energy (vdW  $E$ +electrostatic  $E$ ).

<sup>d</sup>  $\Delta E$  is defined as the difference between the interaction energy of the DM- $\beta$ -CD–paclitaxel complex and the  $\beta$ -CD–paclitaxel complex.

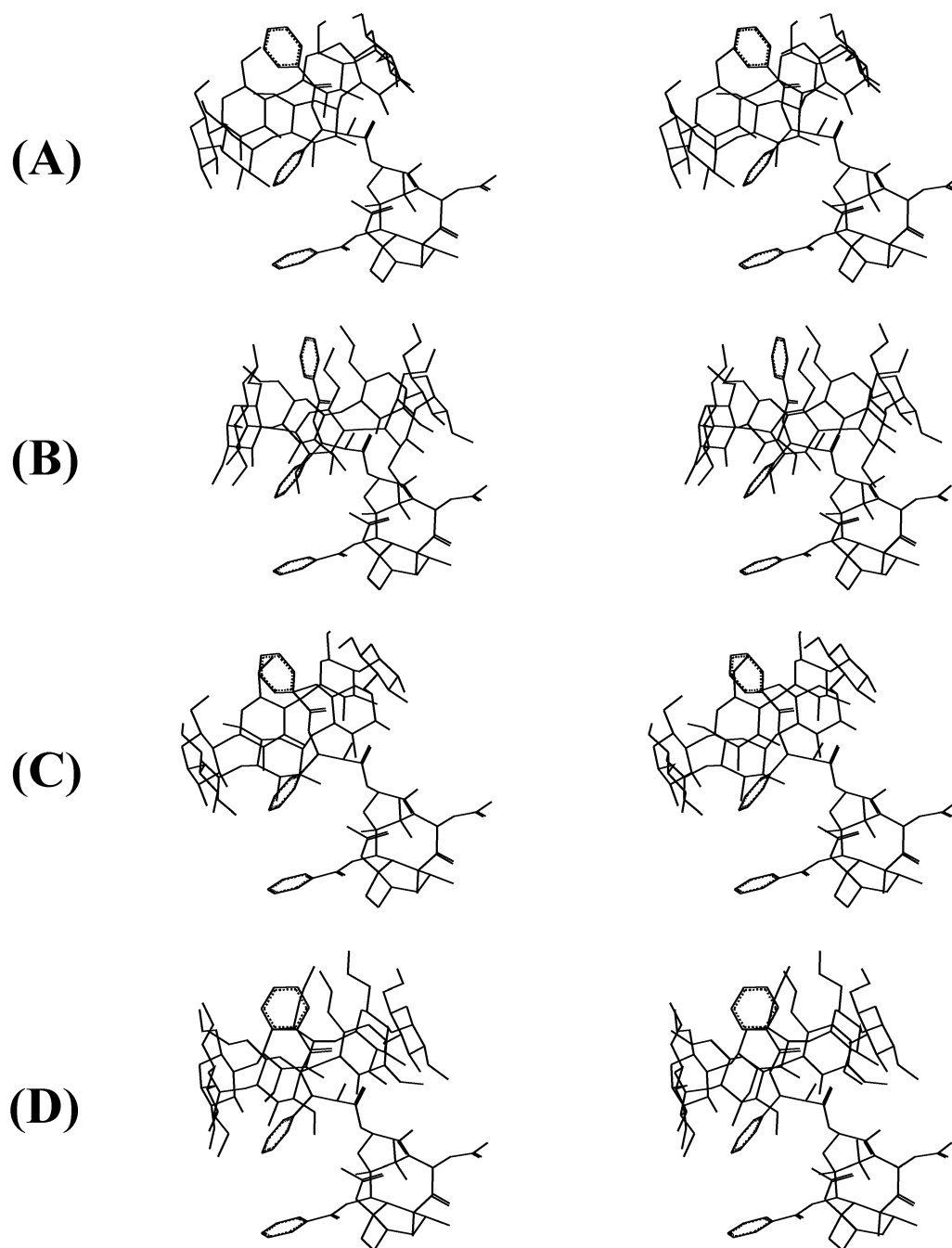


Fig. 4. Stereoview of each of the lowest energy configuration among the inclusion complexes between both CDs and C-3'N benzoyl moiety (B-ring) of paclitaxel. (A)  $\beta$ -CD–paclitaxel complex; (B) DM- $\beta$ -CD–paclitaxel complex in  $\varepsilon = 1$ ; and (C)  $\beta$ -CD–paclitaxel complex; (D) DM- $\beta$ -CD–paclitaxel complex in  $\varepsilon = r$ .

consistent valence force field (CVFF)<sup>18</sup> on a SGI OCTANE 2 workstation (Silicon Graphics, USA).

The molecular model of  $\beta$ -CD was obtained from the crystallographic geometry.<sup>19</sup> The molecular structure of the DM- $\beta$ -CD was derived from the crystal structure of  $\beta$ -CD by modifying the substituents using the builder module within INSIGHTII. The conformational search of DM- $\beta$ -CD was performed by simulated annealing molecular dynamics–full energy minimization strat-

egy,<sup>20,21</sup> and the lowest energy conformation of DM- $\beta$ -CD was selected for the MC docking simulations. The molecular structure of the paclitaxel was obtained from the paclitaxel crystal structure in the Cambridge Database.<sup>22</sup> This structure was energy-minimized until the maximum derivative reached below 0.01 kcal/mol/Å. The H-2'–C-2'–C-3'–H-3' dihedral angle was restrained to 124° according to the proposed torsion angle of the solution structure calculated from the coupling constant

(J) of NMR measurements and MM2 calculation in the published report<sup>16</sup> prior to running the minimization (Fig. 2).

Because the molecular size of paclitaxel is larger than a CD, we regarded the CDs as ligands and the B-ring or HP cluster of paclitaxel as the binding sites of the receptor during the MC docking process. CDs were

positioned to form an inclusion complex with the aid of the docking module of INSIGHTII. The MC docking simulation started by conjugate-gradient energy minimization of this initial configuration for 100 iterations and accepted it as the first frame. The coordinates of both the binding site (B-ring or HP cluster) of paclitaxel and all CDs were made flexible during the MC

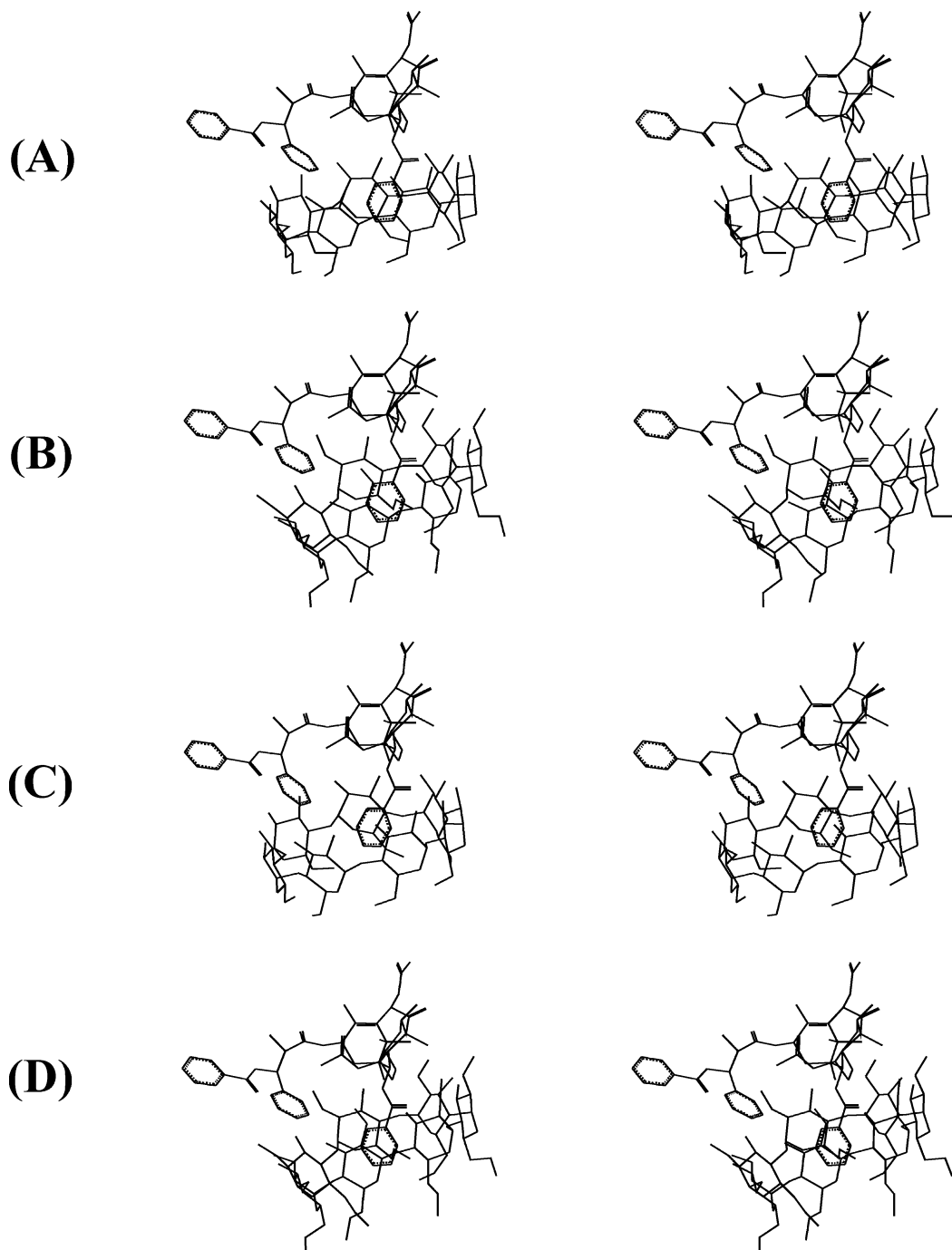


Fig. 5. Stereoview of each of the lowest energy configuration among the inclusion complexes between both CDs and hydrophobic (HP) cluster moiety of paclitaxel. (A)  $\beta$ -CD–paclitaxel complex; (B) DM- $\beta$ -CD–paclitaxel complex in  $\epsilon = 1$ ; and (C)  $\beta$ -CD–paclitaxel complex; (D) DM- $\beta$ -CD–paclitaxel complex in  $\epsilon = r$ . The cavity of DM- $\beta$ -CD more deeply embeds hydrophobic cluster moiety than  $\beta$ -CD.

Table 2

Average distance between host and guest and  $R_G$  of HP cluster site of paclitaxel in HP cluster docking

Dielectric constant	Complexed CDs	Distance (Å)	$R_G$ (Å)
$\epsilon = 1$	$\beta$ -CD	$6.61 \pm 0.31$	$3.74 \pm 0.06$
	DM- $\beta$ -CD	$6.20 \pm 0.17$	$3.83 \pm 0.06$
$\epsilon = r$	$\beta$ -CD	$6.82 \pm 0.29$	$3.70 \pm 0.06$
	DM- $\beta$ -CD	$6.40 \pm 0.20$	$3.83 \pm 0.06$

simulations. But the other geometries of paclitaxel including the H-2'-C-2'-C-3'-H-3' dihedral angle were restrained to the initial conformation.

Trials to a new configuration were accomplished by changing the position and orientation of the CDs. In this process, the CDs could take translational movement to the  $x$ ,  $y$ , and  $z$  axes (maximum 1 Å) and rotation around the  $x$ ,  $y$ , and  $z$  axes (maximum 180°). Six degrees of freedom were present for this system (three translational and three rotational). Trial began with a random change of up to 5 degrees of freedom among them. If the energy of the resulting configuration was within 10,000 kcal/mol from the last accepted one, it was subjected to the 100 iterations of conjugated gradient energy minimization. The energy tolerance of 10,000 kcal/mol was imposed to avoid significant overlap of van der Waals radii in the random search. After the energy minimization, acceptance was determined by the following two criteria: (a) An energy check with the Metropolis criteria at 300 K;<sup>23</sup> and (b) a root-mean-squared displacement (RMSD) check, which compared the RMSD of the new configuration against those accepted so far. Configurations within 0.1 Å RMSD of preexisting ones were discarded to avoid accepting similar configurations. The next trial began like the above procedure. The MC docking simulations continued until there was complete energy convergence. No cutoff was imposed on the calculation of nonbonded interactions, and the dielectric constant was set to 1 in vacuo or  $r$  in the implicit solvent for the electrostatic interaction.<sup>17</sup>

## Acknowledgements

We are grateful for Dr Arthur Camerman, AR-DONO Research, Seattle, USA, for providing the paclitaxel coordinates for this research. This work was

supported by grants of the Bioproducts and Biotechnology Research Group (01-J-BP-01-B-59) from the Ministry of Science and Technology in South Korea (SDG).

## References

- Wani, M. C.; Taylor, H. L.; Wall, M. E.; Coggon, P.; McPhail, A. T. *J. Am. Chem. Soc.* **1971**, *93*, 2325–2327.
- Donehower, R. C.; Rowingsky, E. K.; Grochow, L. B.; Longnecker, S. M.; Ettinger, D. S. *Cancer Treat. Rep.* **1987**, *71*, 1171–1177.
- Rowinsky, E. K.; Cazenave, L. A.; Donehower, R. C. *J. Natl. Cancer Inst.* **1990**, *82*, 1247–1259.
- Suffness, M. *Annu. Rep. Med. Chem.* **1993**, *28*, 305–314.
- Sharma, U. S.; Straubinger, R. M. *Pharm. Res.* **1994**, *11*, 889–896.
- Waugh, W. N.; Trissel, L. A.; Stella, V. J. *Am. J. Hosp. Pharm.* **1991**, *48*, 1520–1544.
- Sharma, U. S.; Balasubramanian, S. V.; Straubinger, R. M. *J. Pharm. Sci.* **1995**, *84*, 1223–1230.
- Lee, S.; Seo, D.-H.; Kim, H.-W.; Jung, S. *Carbohydr. Res.* **2001**, *334*, 119–126.
- Pitha, J.; Milecki, J.; Fales, H.; Pannell, L.; Uekama, K. *Int. J. Pharm.* **1986**, *29*, 73–82.
- Brewster, M.; Hora, M.; Simpkins, J.; Bodor, N. *Pharm. Res.* **1991**, *8*, 792–795.
- Heindel, N. D.; Eglolf, R. A.; Stefely, J. S. *J. Pharm. Sci.* **1990**, *79*, 862–865.
- Brewster, M.; Loftsson, T.; Estes, K.; Lin, J.-L.; Fridriksdottir, H.; Bodor, N. *Int. J. Pharm.* **1992**, *79*, 289–299.
- Szejtli, J. *Pharm. Technol. Int.* **1991**, *3*, 15–22.
- Hamada, H.; Saito, K.; Mikuni, K.; Kuwahara, N.; Takahashi, H. US Patent 5 684 169, 1997; *Chem. Abstr.* **1997**, *128*, 7318.
- Kwon, C.; Choi, Y.-H.; Kim, N.; Yoo, J.-S.; Yang, C.-H.; Kim, H.-W.; Jung, S. *J. Incl. Phenom.* **2000**, *36*, 55–65.
- Ojima, I.; Kuduk, S. D.; Chakravarty, S.; Ourevitch, M.; Begue, J.-P. *J. Am. Chem. Soc.* **1997**, *119*, 5519–5527.
- (a) Luty, B. A.; Wasserman, Z. R.; Stouten, P. F. W.; Hodge, C. N.; Zacharias, M.; McCammon, J. A. *J. Comp. Chem.* **1995**, *16*, 454–464;  
(b) Widmalm, G.; Venable, R. M. *Biopolymers* **1994**, *34*, 1079–1088.
- Dauber-Osguthorpe, P.; Roverts, V. A.; Osguthorpe, D. J.; Wolff, J.; Genest, M.; Hagler, A. T. *Proteins: Struct. Funct. Genet.* **1988**, *4*, 31–47.
- Betzel, C.; Saenger, C.; Hingerty, B. E.; Brown, G. M. *J. Am. Chem. Soc.* **1984**, *106*, 7545–7550.
- Choi, Y.-H.; Kang, S.; Yang, C.-H.; Kim, H.-W.; Jung, S. *Bull. Korean Chem. Soc.* **1999**, *20*, 753–756.
- Beier, T.; Holtje, H.-D. *J. Chromatogr. B.* **1998**, *708*, 1–20.
- Mastropaolo, D.; Camerman, A.; Luo, Y.; Brayer, G. D.; Camerman, N. *Proc. Natl. Acad. Sci. USA* **1995**, *92*, 6920–6924.
- Metropolis, A. W.; Rosenbluth, M. N.; Rosenbluth, A. H.; Teller, E. *J. Chem. Phys.* **1953**, *21*, 1087–1092.